Characterization of epigenetic modification of exosomal DNA and its clinical application

DooA Kim

Department of Medical Science

The Graduate School, Yonsei University

Characterization of epigenetic modification of exosomal DNA and its clinical application

DooA Kim

Department of Medical Science

The Graduate School, Yonsei University

Characterization of epigenetic modification of exosomal DNA and its clinical application

Directed by Professor Han Sang Kim

The Master's Thesis
submitted to the Department of Medical Science,
the Graduate School of Yonsei University
in partial fulfillment of the requirements for the degree of
Master of Medical Science

DooA Kim

December 2020

This certifies that the Master's Thesis of
DooA Kim is approved.

_____
Thesis Supervisor: Han Sang Kim

_____
Thesis Committee Chair: Joong Bae Ahn

_____
Thesis Committee Member: Tae-Gyun Kim

The Graduate School
Yonsei University

December 2020

ACKNOWLEDGEMENTS

My appreciation goes first to Professor Han Sang Kim, who guided me throughout my master's degree program over the past two years. His enthusiasm for science motivated me and kept me engaged with my research, constantly.

I thank my thesis committee chair and member, Professor Joong Bae Ahn and Professor Tae-Gyun Kim for taking their precious time to evaluate my thesis. I also thank my laboratory colleagues. Especially, Dr. Kyung-A Kim's mentoring and encouragement has helped me to finish my master's program.

Most of all, I am deeply grateful for my family, friends and love. Thanks to my parents, who are my greatest supports of all time. My gratitude extends to my sister my cousin, and my love who helped me to survive from all the stress, comforted me with warm words, and cheered me up when I was at my lowest point. I cannot thank enough.

Finally, I thank God for everything.

TABLE OF CONTENTS

LIST OF FIGURES

ABSTRACT

Characterization of epigenetic modification of exosomal DNA
and its clinical application

DooA Kim

Department of Medical Science
The Graduate School, Yonsei University

(Directed by Professor Han Sang Kim)

Exosomes are 30-150 nm-sized endosomal derived extracellular vesicles implicated in intercellular communication and transfer of genetic information. Exosomes contain various types of nucleic acids, including double stranded-DNA. Although aberrant DNA methylation changes can be useful cancer biomarker for cancer detection, epigenetic characterizations of exosomal DNA is still elusive. In this study, we performed genome-wide methylation profiling using Infinium MethylationEPIC BeadChip to interrogate the methylation status of 853,307 CpG sites of nuclear, cytoplasmic, and exosomal DNA derived from MDA-MB-231 and HCT-116 cancer cell-lines, respectively. Hierarchical clustering of methylation profiles based on nearby CGI segregated three categories (islands, shelf, and shore) showed that the methylation profiles among different cellular fractions are mostly concordant. Of note, the DNA methylation pattern is comparable between nuclear and exosome. The Pearson correlation coefficient was 0.98 (HCT-116) and 0.99 (MDA-MB-231) between nuclear DNA and exosomal DNA, suggesting that methylation analysis of exosomal DNA derived from cancer cells can be applicable for cancer detection. Further analysis is necessary to clarify the role of exosomal DNA with epigenetic modification in the tumor microenvironment.

Key words: exosome, epigenetics, DNA methylation

Characterization of epigenetic modification of exosomal DNA and its clinical application

DooA Kim

Department of Medical Science
The Graduate School, Yonsei University

(Directed by Professor Han Sang Kim)

I. INTRODUCTION

Exosomes are 30-150 nm sized extracellular vesicles secreted by multi-vesicular bodies [1]. Exosomes are gaining growing reputation for their roles in cellular homeostasis, immune response and intercellular communication [2]. Exosomes transfer biomolecules between the cells via membrane vesicle trafficking. Molecules that are delivered by exosome contain lipid, protein, and nucleic acids including DNA [3]. DNAs in exosomes are mainly double-stranded [4] and they exhibit characteristics of originated cells and represent the entire genome and the mutational status of parental tumor cells [5]. Because exosomal DNA represents its cell of origin and due to the fact that exosomes can be found in various types of body fluids including blood [6] and urine [7], many researches on applying exosomal DNA in a liquid biopsy have been conducted [8 9]. In contrast to emerging attention on exosomal DNA, not many studies on epigenetic characteristics of exosomal DNA have been done yet because of relatively low amount DNA existing in exosome.

Epigenetic modifications such as DNA methylation, histone modification, and RNA interference enable proper gene regulation in normal cells and lead appropriate development and maintenance of gene expression level in mammals [10]. Failure of proper epigenetic processes causes various diseases including cancer [11]. Numerous evidences of abnormalities in epigenetic modification linking with cancer were discovered through various studies. Of all abnormalities, DNA methylation is one of the most intensely studied epigenetic alterations in cancer [12].

Aberrant DNA methylation in cancer affects regulation of gene expression and transcriptional repression [13]. Hypermethylation of the promoter region leads inactivation of tumor suppressor genes while global hypomethylation induces genomic instability and causes cell transformation [14]. These alterations were first observed in specific genes in human colon cancer cells in comparison to normal cells [15] and sequentially in many other types of cancer in later studies.

These studies suggest that aberrant pattern of DNA methylation in exosome derived from cancer cells can be applied as a useful biomarker for cancer detection. Moreover, studying epigenetic characteristic of exosomal DNA is important to understand disease progression after genetic information transmission. In this study, we characterized pattern of DNA methylation in exosome via genome-wide methylation profiling. Global and local DNA methylation pattern of exosomal DNA was also investigated and compared to genomic DNA.

II. MATERIALS AND METHODS

1. Sample preparation

Cell lines and culture

Two types of cancer cell line, HCT-116 (HCT116) and MDA-MB-231 (MDA231) were used in this experiment. HCT-116 and MDA-MB-231 cell lines were obtained from ATCC. Cells were cultured in Hyclone DMEM with high glucose supplemented with 10% fetal bovine serum (FBS) and 1% penicillin/ streptomycin and incubated at 37 ℃ in 5% CO_2 humidify atmosphere.

Tissue samples

Fresh human tumor tissues were obtained from patients by surgeries conducted at Yonsei Cancer Center (YCC). Tumor tissues of two patients were collected in ice-cold phosphate-buffered saline (PBS).

2. Cell fractionation

Nuclear and cytosolic fractions from HCT116 and MDA231 cells were performed by using Pierce Mitochondria Isolation Kit for Cultured Cells (Thermo Fisher Scientific, Waltham, MS, USA). Fractionation steps were followed by the manufacturer's instruction.

3. Isolation of Exosome

From culture media

HCT116 and MD231 cells were maintained in exosome depleted DMEM/ high glucose media supplemented with 10% fetal FBS and 1% penicillin/ streptomycin

and were incubated in 5% CO_2 at 37 ℃. After 72 hours, culture media were collected and centrifuged at 500 x g for 10 minutes to remove the cells. Additionally, supernatant of the media was centrifuged at 3,000 x g for 20 minutes to remove the dead cells and cell debris. Supernatant was collected and transferred to ultra-clear tubes in 70Ti rotor and was ultra-centrifuged at 12,000 x g for 20 minutes at 4 ℃. Subsequently, supernatant was collected and transferred into fresh ultracentrifuge tubes, then ultra-centrifuged at 100,000 x *g*, at 4 ℃ for 70 minutes. Supernatant was discarded and pallets were suspended with 1 mL PBS. Suspended pallets were centrifuged at 100,000 x *g*, at 4 ℃ for 70 minutes. At last, the PBS was removed and isolated exosome enriched pallets were eluted with 200 μL of PBS.

From tissue samples

Tissues collected in PBS were washed with PBS three times and cut into appropriate sized pieces in a 6 well plate. Pieces of tissues were cultured in RPMI supplemented with 1% penicillin/ streptomycin and incubated at 37 ℃ in 5% CO_2 humidify atmosphere for 7 to 10 hours. Tissue culture media were collected and the exosome were isolated by differential ultra-centrifugation method as described above in isolation of exosome from cell culture media.

4. Exosome Characterization

Western blot analysis

To quantify protein concentration of isolated exosomes, each sample was mixed with lysis buffer and incubated in ice for 30 minutes. 30 μg of protein was suspended

in 5X sample buffer and boiled for 3 minutes at 95 ℃. Proteins were separated by SDS-PAGE and transferred to polyvinyldene fluoride membranes, blocked in 5% skim milk in PBS with 0.5% Tween-20. Immune-staining was performed with primary antibodies; Lamin B1 (nuclear envelope marker; Cell Signaling Technology, Cat. 2118S), Beta-actin (cytoskeletal protein marker; Cell Signaling Technology, Cat. 12262S), GAPDH (loading control; Cell Signaling Technology, Cat. 12586), CD9 (exosome marker; Novus Biologicals, NBP2-22187) and secondary antibodies consecutively. Then, separated proteins were treated with enhanced chemiluminescence (ECL) buffer and detected using Chemi-luminescent Image Analyzer (ImageQunat LAS 4000 mini, Fuji Film, Tokyo, Japan).

Nanoparticle tracking analysis (NTA)

To evaluate the concentration and size distribution of exosome particles, isolated exosomes were recorded using NanosSight NS300 microscope (NanoSight LTD., Amesbury, UK) equipped with a 405 nm laser. 60 seconds video of each sample was recorded three times with detection threshold set at 3. Videos recorded for each sample were analyzed with NTA software (version 2.3; NanoSight LTD.).

5. DNA preparation and evaluation

Genomic DNA

Total DNA, nuclear DNA, cytosolic DNA were isolated using QIAamp DNA Mini Kit, QIAGEN (Catalogue No. 51304). DNAs were extracted by the manufacturer's instruction and quantified using Nanodrop (Thermo Scientific, Waltham, MA, USA).

The size of double stranded DNA was analyzed by 4200 TapeStation system (Agilent Technologies, Santa Clara, CA, USA) and DNA High sensitivity kit (Agilent Technologies, Santa Clara, CA, USA).

Exosomal DNA

DNAs from exosomes were isolated using magnetic bead DNA isolation method. 200 μL of AL lysis and 10 μL of proteinase K were added to enriched exosome with 200 μL of PBS. Then, samples were placed in heat block for 10 minutes, at 56 ℃. 200 μL magnetic beads (AMPure™ XP, Beckman-Coulter, Brea , CA, USA), 200 μL PEG NaCl solution, and 200 μL ISO-propanol were added to the sample tubes and incubated in room temperature for 5 minutes. Then, sample tubes were placed in magnetic bar until beads were attached to the wall. Samples were washed twice with 80% ethanol. After ethanol was subtracted, sample tubes were dried in the room temperature for 5 minutes. Finally, beads were eluted with 20 μL of ddH2O and stored in -20 ℃. The concentration and purity of DNA derived from exosomes were assessed by Qubit and the size of double-stranded DNA was detected using 4200 TapeStation System (Agilent Technologies) and DNA High sensitivity kit (Agilent Technologies).

6. Methylation profiling

Methylation profiling was performed using microarray-based platforms of Infinium MethylationEPIC BeadChip designed to interrogate the methylation status of 853,307 CpG sites (Illumina Inc., San Diego, CA, USA). The resulting raw data

(IDAT files) were processed using GenomeStudio software and R packages. For background correction, the background intensity was estimated from a set of negative controls and extracted from the fluorescent signals of M (methylated) and U (unmethylated) alleles at each analytical data point. Dye bias equalization was employed for the background corrected intensities. The ratio of processed signals was computed from the signals of two alleles with a formula, beta-value = (max(M, 0))/(|U| + |M| + 100) reflecting the methylation level of each CpG site. We further normalized the values using beta-mixture quantile (BMIQ) normalization. Normalized methylation profiles were prepared for 2 cell lines and four cellular fractions and used for the subsequent analyses. The relative abundance of CpGs were investigated with respect to the feature categories of gene region (i.e., TSS200, TSS1500, 5'UTR, 1st Exon, Body, and 3'UTR) and CpG islands (island, shore and shelf).

7. Validation of methylation status by pyrosequencing.

DNA methylation level of particular CpG sites of candidate probes was quantified by pyrosequencing. A primer set is shown in **Supplementary Table 3**. Pyrosequencing reactions and quantification of DNA methylation were run on PyroMark Q48 Autoprep pyrosequencing system (QIAGEN, Valencia, CA, USA).

8. Clustering and functional analysis

Hierarchical clustering was done using the Euclidian distance between BMIQ normalized beta-values of cell lines and cellular fractions with a complete linkage.

One-hundred with large difference and one-hundred with low difference between exosome and nucleus DNA s were extracted from each cell lines, gene-set enrichment analysis (GSEA) was performed by Fisher's exact test in R. In case of having multiple genes in one CpG probe, gene in region that further affect gene expression was selected. The beta-value of CpG sites compared with human mammary epithelial cells (HMEC) from ChromHMM, chromatin states corresponding to CpG sites were determined.

III. RESULTS

1. Identification and characterization of exosome from culture media

To verify exosome isolation method, we characterized the exosomes by western blot analysis. The presence of exosomal protein marker (CD9) was observed in the samples, whereas nuclear envelope marker, Lamin B1, was only detected in nuclear fractions (**Fig. 1C**). In addition, each exosome samples were analyzed with nanoparticle tracking analysis (NTA) which characterized the size and concentration of exosomes (**Fig. 1B**). Particles with diameters from 30 to 150 nm were detected over 80 % of all particles with a mean size of 119, 121 nm in each cell-line derived samples. Western blot analysis and Nanoparticles tracking analysis indicate that preparation samples exhibit the characteristics of exosome.

2. Features of exosomal DNA

Total exosomal DNA derived from HCT116 and MDA231 were characterized using High sensitive DNA ScreenTape in a 4200 TapeStation System (Agilent Technologies). The main exosomal DNA peaks in HCT116 and MDA231 were detected around 7 kb and 10 kb (**Fig. 1E**)

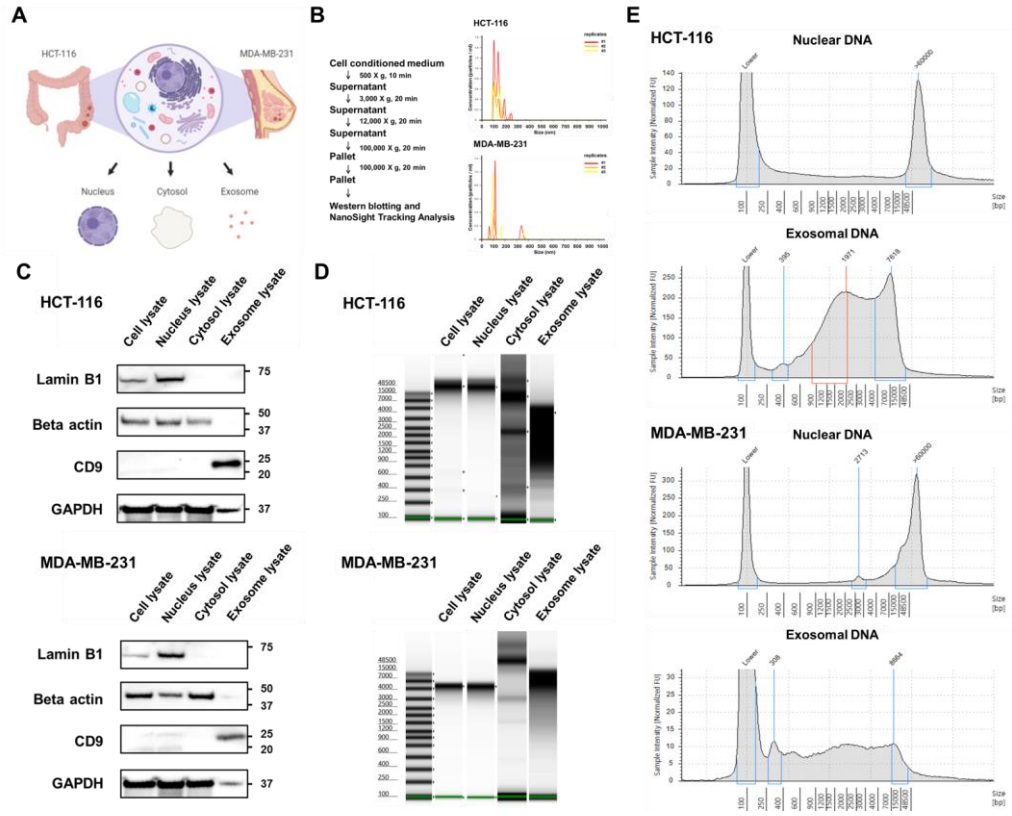

Figure 1. **Characteristics of Exosome and Exosomal DNA.** (**A)** Nucleus, Cytosol, Exosome isolation from two cell lines: HCT-116 and MDA-MB-231. (**B)** Exosome isolation process using ultracentrifuge and NanoSight Tracking data. (**C)** Western blot analysis of cell fractions from each cell lines. (**D)** Gel image of Nuclear DNA, Mitochondrial DNA, Cytosolic DNA, Exosomal DNA. (**E)** Electro-phenogram image of nuclear DNA and exosomal DNA of each cell lines.

3. Distributions of beta-values for two cell lines

Genomic DNAs were obtained from MDA231 and HCT-116, human breast cancer and colorectal cancer cell lines, for four cellular fractions including exosomal DNAs along with DNAs from nucleus, cytosol and whole cell lysates. Beadarray-based CpG methylation profiling was done for genomic DNAs to interrogate the methylation statues of 850,000 CpGs. (**Fig. 2A)** shows the distribution of normalized beta-values for two cell lines and four cellular fractions. Bimodal peaks representing the hypo- and hyper-methylated CpGs were consistently observed across the cell lines and cellular fractions. But we also noted heterogeneity between cell lines and cellular fractions, e.g., for MDA231, hypomethylated CpGs were enriched compared to HCT-116 indicative of cell line-specific heterogeneity of DNA methylation profiles. In addition, cytosolic DNAs of both cell lines uniquely showed an elevation of the intermediate level of methylation (arrows, **Fig. 2A**).

CpG markers were further classified with respect to nearby CpG islands (islands, N-/S-Shore, N-/S-shelf) and examined for their level of methylation. CpGs were differentially methylated with respect the CpG islands, i.e., hypomethylated CpGs were dominant over hypermethylated CpGs within CpG islands compared to those outside CpG islands. And CpGs outside CpG islands are responsible for the elevation of the intermediate level of methylation for cytosolic DNA. Hierarchical clustering of the densities of hypo- and hypermethyated CpGs also demonstrates that the methylation patterns with respect to the CpG islands (i.e., dominance of hypo- and

hyper-methylated CpGs of CpG islands and shelf, respectively) are dominant over the difference between the cell lines or between the cellular fractions (**Fig. 2B**). Individual histrograms with respect to the cell lines and cellular fractions are available in (**Supplementary Fig. 1A)**. CpG markers annotated with respect to nearby genes also showed that TSS1500, TSS200 and 1st Exon-residing CpGs are enriched with hypomethylated CpGs compared to those in gene bodies (**Fig. 2C**). Individual histograms are also shown in (**Supplementary Fig. 2)** demonstrating that the relationship with nearby genes is dominant over the cell line or cellular fractions.

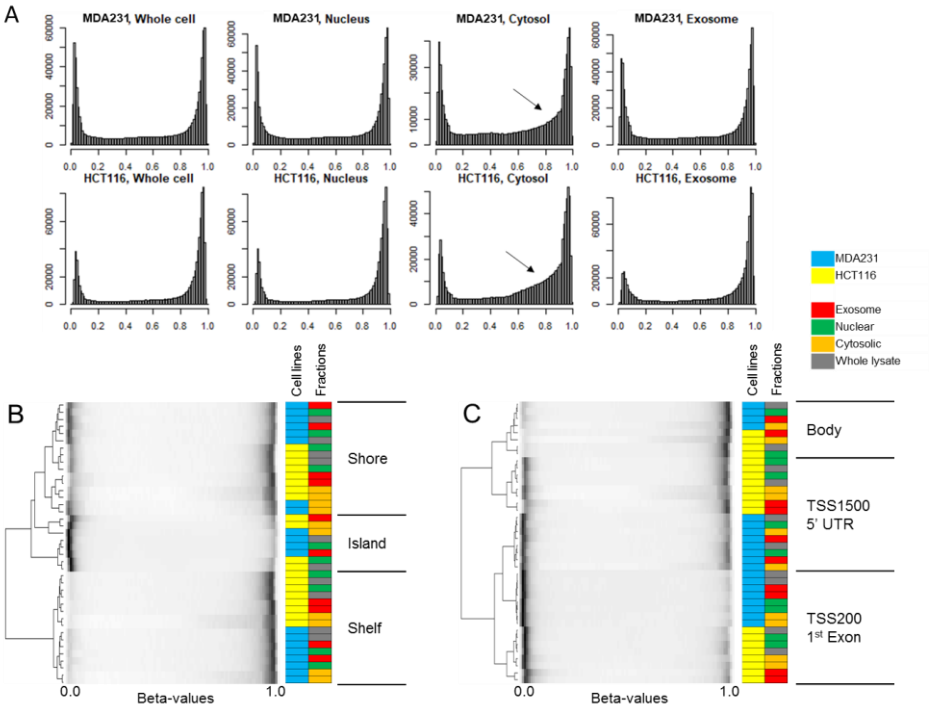

Figure 2 Methylation level with respect to the cellular fractions. (A) For two cell lines, the normalized beta-values are shown for their distribution in four cellular fractions. **(B)** Hierarchical clustering of beta-values.

4. Concordance of DNA methylation between exosome-derived and nuclear DNA

Fig. 3A shows the hierarchical clustering of the examined methylation profiles segregated the two cell lines highlighting a substantial level of heterogeneity between cell lines. In both cell lines, DNAs from nucleus, whole cell lysates and exosomes were co-segregated while cytosomal DNAs were identified as outliers consistent with methylation density distribution (**Fig. 2A**). Pairwise correlation heatmaps are provided in (**Fig. 3B)**. **Supplementary Fig. 3** shows that the segregating patterns across the cellular fractions are consistent across CpG categories with respect to nearby genes and CpG islands. To delineate the epigenetic changes acquired by exosomal DNAs during the transit from the nucleus, we focused on the CpGs that are differentially methylated between exosomal and nuclear DNAs. Substantial level of correlation between nuclear and exosomal DNAs are shown for two cell lines (Pearson correlation coefficient of 0.997 and 0.991 with *P* values of 0 and 0 for MDA231 and HCT116, respectively; **Fig. 3C** and **D**).

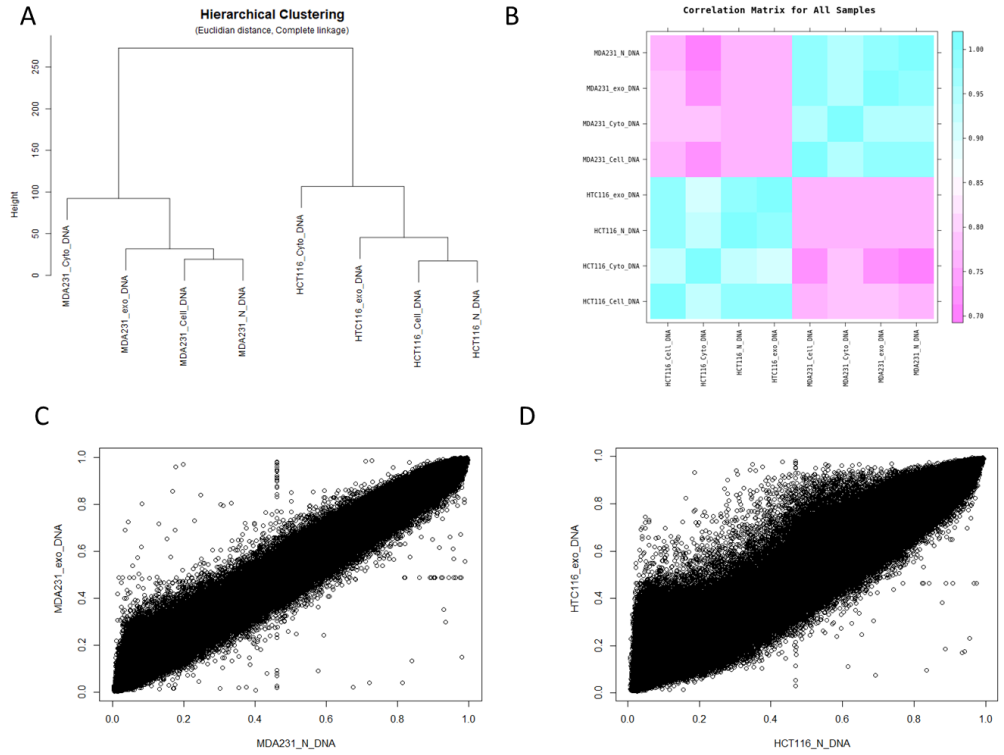

Figure 3. Concordance of DNA methylation levels across cellular fractions. (A) Hierarchical clustering of the examined methylation profiles. (B) Pairwise correlation heatmaps. (C, D) Substantial level of correlation between nuclear and exosomal DNAs are shown for two cell lines. (Pearson correlation coefficient of 0.997 and 0.991 for MDA231 and HCT116, respectively.)

5. Functional enrichment analysis of differential methylation levels

To identify the molecular functions coordinated by the exosome-specific epigenetic changes, we first selected genes harboring CpGs with differential of beta-values between exosomal and nuclear DNAs. PreRanked gene-set enrichment analysis (GSEA) results are shown in **Supplementary Fig. 4** and **Supplementary Table 1**. We next selected top and bottom 100 genes in the extreme of differentials for each of two cell lines. Fisher's exact test with Gene Ontology (GO) molecular terms revealed that the CpGs hypermethylated and hypomethylated in exosomes of MDA231 and HCT116 are enriched in genes with a function representing nucleoplasm and cytosol, respectively (**Supplementary Table 2**).

6. Genomic features associated with exosomal DNA methylation

To further figure out the epigenetic configuration vulnerable to the exosomal DNA, we performed enrichment analysis of CpG sites with respect to ENCODE chromatin states segmentation by ChromHMM. **Fig. 4A** and **B** shows the relative abundance of hyper- and hypomethylated CpGs of exosomal DNA with respect to 15 ChromHMM states representing unique epigenetic configurations. We observed that the proportion of hypermethylation is higher in 1_Active_Promoter (active promoter), whereas the proportion of hypomethylation is higher in 10_Txn_Elongation (transcription elongation). In particular, the hypermethylated CpG sites were overrepresented on transcription related configurations (9_Txn_Transition (transcription translocation),

10_Txn_Elongation, 11_Weak_Txn (weak transcription)). Using the differential beta values between exosomal and nuclear DNAs, we also observed that the CpGs resident in 1_Active_Promoters are significantly enriched in exosomal DNAs suggesting that the exosomal DNAs are more hypermethylated in genomic regions marked as '1_Active_Promoter'. CpGs more methylated in nuclear DNAs than exosomal DNAs were instead enriched in '10_Txn_Elongation'

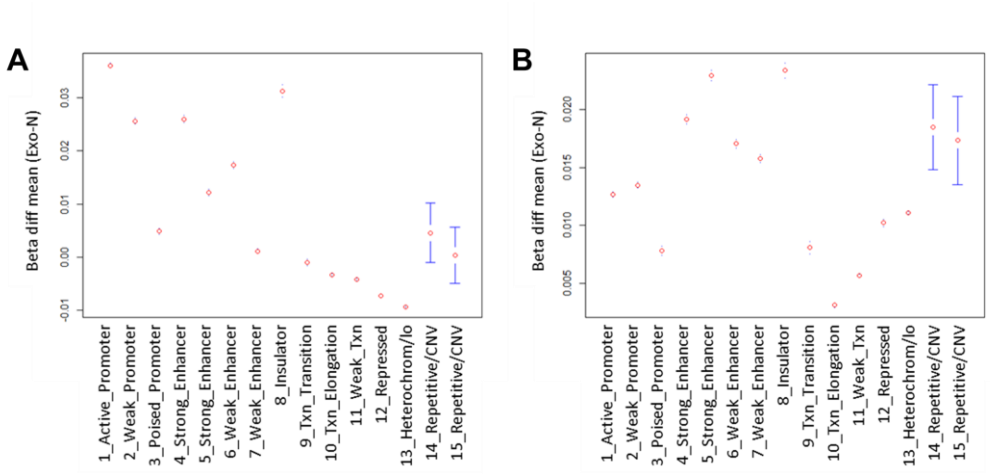

Figure 4. Relative abundance of hyper- and hypo-methylated CpGs of exosomal DNA. (A, B) Relative abundance of hyper- and hypo-methylated CpGs of exosomal DNA with respect to 15 ChromHMM states represents unique epigenetic configurations

7. Experimental validation

For experimental validation, we calculated three-probe moving average of the differentials between exosomal and nuclear DNAs. Candidate probes with highest scores were cg15696408, cg20305912, cg14017196 in HCT116 and cg00490885, cg21653586, cg23984434 in MDA231. Five probes except cg23984434 were observed to be correlated with flanking probes. Although cg23984434 was not shown correlated methylation pattern with flanking probes, cg21653586 was consistent with that found in the analysis based on hyper- and hypo-methylation (**Fig. 5B**). These probes were used for subsequent experimental validation by pyrosequencing. Among listed candidate probes, DNA methylation status of two candidate probes (cg15696408, cg00490885) was detected by pyrosequencing. Different methylation level of candidate exosomal DNA probe compared to genomic DNA probe is shown in **Fig. 5C, D.**

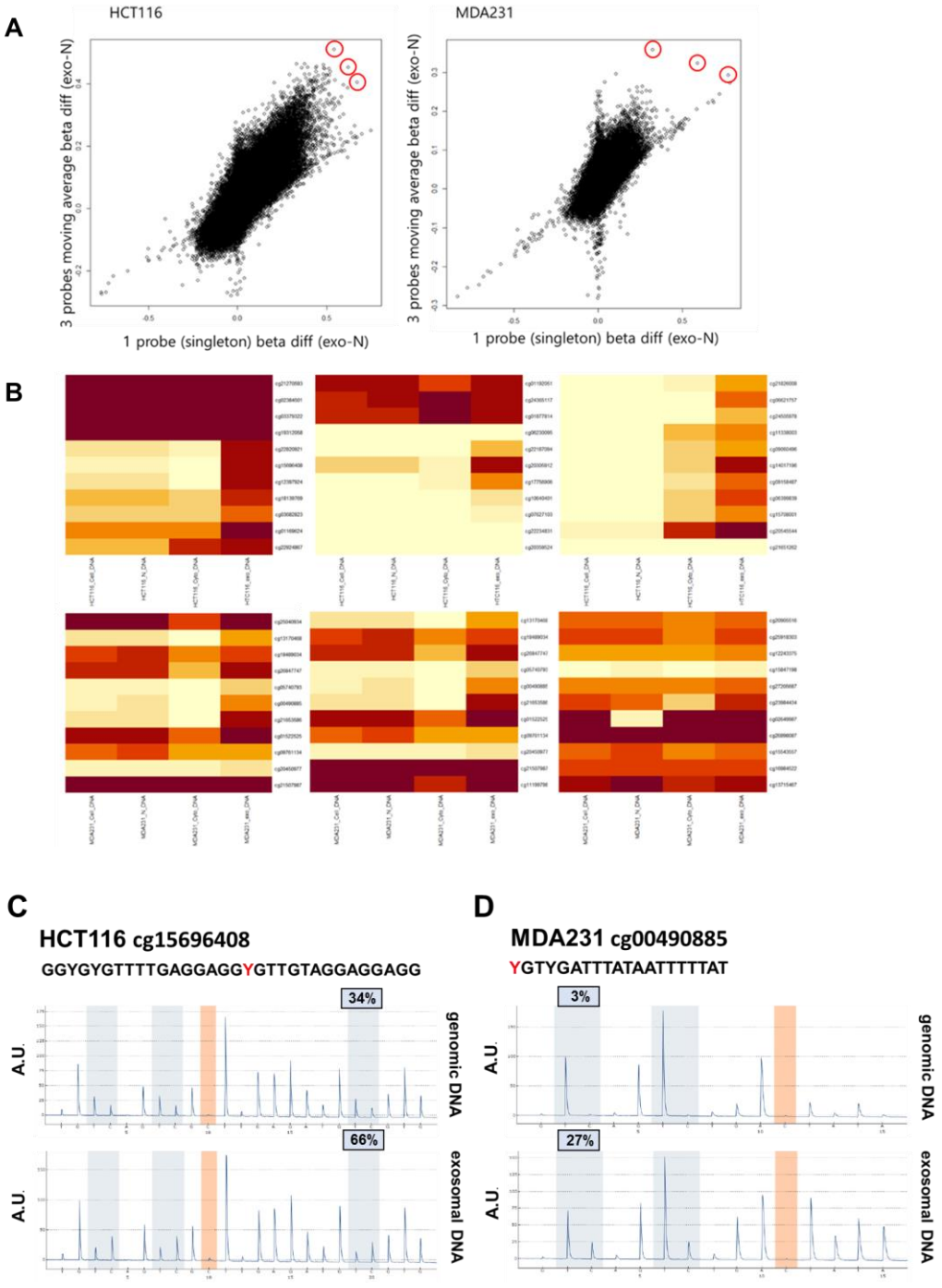

Figure 5. Correlation between exosomal and nuclear DNA. (A) Correlation with

flanking probes marked with red circles. (B) Heatmaps of candidate probes (cg15696408, cg20305912, cg14017196 in HCT116 and cg00490885, cg21653586, cg23984434 in MDA231). (C, D) Pyrograms of DNA isolated from nucleaus and exosome from each cell-line (cg15696408, cg00490885)

8. Concordance of DNA methylation between Human tissue derived exosomal DNA and genomic DNA

Fig. 5A shows the hierarchical clustering of the examined methylation profiles segregated the two tumor tissues highlighting a substantial level of heterogeneity between tissue and tissue derived exosome. In both patients, DNAs from tissues and exosomes were co-segregated. Pairwise correlation heatmaps are provided in (**Fig. 5B)**. Substantial level of correlation between genomic and exosomal DNAs are shown for two cell lines (Pearson correlation coefficient of 0.96 and 0.94 with *P* values of 0 and 0 for genomic DNA and exosomal DNA of two tissue samples, respectively; **Fig. 5C**).

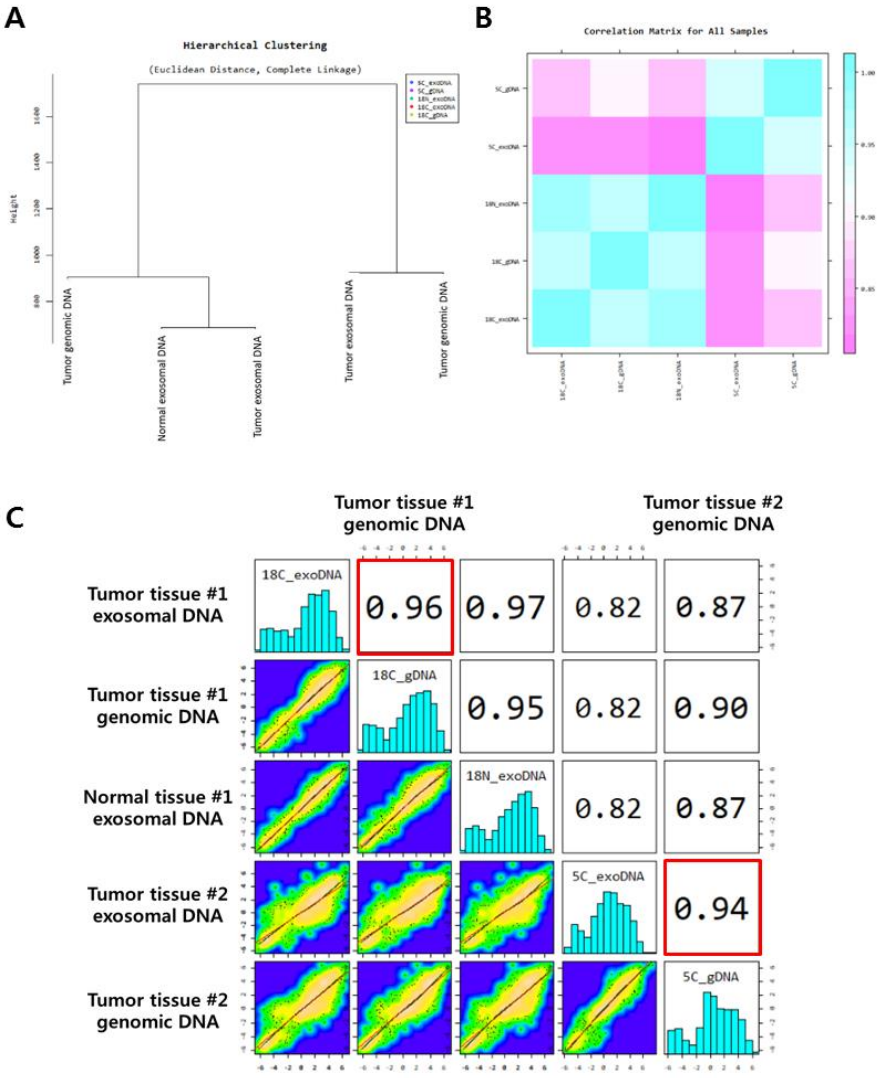

Figure 5

. Concordance of DNA methylation levels across tissue derived exosomal DNA and genomic DNA. (A) Hierarchical clustering of the examined methylation profiles. (B) Pairwise correlation heatmaps. (C) Substantial level of correlation between nuclear and exosomal DNAs are shown for two cell lines. (Pearson correlation coefficient of 0.96 and 0.94)

IV. DISCUSSION

Cancer is a foremost cause of death worldwide, accounting for an estimated more than 9 million deaths each year according to World Health Organization. In most of the cases, primary cancers can be cured by surgical procedures and proper treatments. However, metastatic cancers are difficult to treat and are the reason of 90% cancer-related deaths. Late diagnosis of cancer usually indicates metastasis of cancer which makes it challenging to treat, thus reducing patients' survival rate. Therefore, early diagnosis of cancer is the key to improve patients' chances of survival.

Researches on the genetic and epigenetic characteristics of exosomal DNA have increased greatly over the past years due to its advantages over existing source of DNA for diagnostic purpose [16] [17]. In our study, methylation level of exosomal DNA was analyzed and compared with nuclear DNA from two types of cancer cells. Our results showed concordant methylation profiles among nuclear DNA and exosomal DNA which indicate exosomal DNA as cell's avatar and propose possible clinical application in cancer detection. Our research also demonstrated local differences of methylation level between nuclear DNA and exosomal DNA.

Potential application on clinical utility of nucleic acids in exosome is receiving growing attention. Further analysis is needed to be done to clarify whether exosome contain tumor-related methylated DNA that reflects the methylation status of nuclear DNA. Furthermore, there are some limitations in our study. Exosomes from human plasma contained low amount of DNA, therefore was unable to be applied for

Infinium MehtylationEPIC BeadChip method. New approaches need to be developed to enrich exosome DNA from human plasma samples.

V. CONCLUSION

In this study, we compared DNA methylation of Nuclear DNA and Exosomal DNA from the cell lines. We used ultracentrifugation method to isolate exosomes which has been verified in previous studies. Validation of exosome was performed by Western blot and Nanoparticle Tracking Assay. Western blotting showed that exosome express the exosomal marker CD9 protein; Nanoparticle tracking assay characterized exosome particle size and concentration. Features of exoDNA derived from each cell lines were examined and double-stranded DNA fragments at the size of 7~10 kb were detected.

Exosomal DNA is comparable to nuclear DNA. To test this, we extracted DNA from the culture media of two cell lines and also DNA from cytosol and nucleus of each cell lines. We applied genome-wide methylation profiling via Infinium MehtylationEPIC BeadChip method to compare the level of DNA methylation. Hierarchical clustering of methylation profiles based on nearby CGI segregated three categories (islands, shelf, and shore) showed concordant methylation profiles among different cellular fractions. The Pearson correlation coefficient of HCT116 and MDA231 was 0.98 and 0.99 between nuclear DNA and exosomal DNA, respectively.

Based on our observations in cell lines, we assumed that DNA methylation level of human tissue derived exosome may also be comparable to tissue derived genomic DNA. Our results suggest that methylation analysis of exosomal DNA derived from cancer cells can be applicable for cancer detection.

REFERENCES

1. Raposo G, Stoorvogel W. Extracellular vesicles: exosomes, microvesicles, and friends. J Cell Biol 2013;200:373-83.

2. Takahashi A, Okada R, Nagao K, Kawamata Y, Hanyu A, Yoshimoto S, et al. Exosomes maintain cellular homeostasis by excreting harmful DNA from cells. Nat Commun 2017;8:15287.

3. Thery C, Zitvogel L, Amigorena S. Exosomes: composition, biogenesis and function. Nat Rev Immunol 2002;2:569-79.

4. Thakur BK, Zhang H, Becker A, Matei I, Huang Y, Costa-Silva B, et al. Double-stranded DNA in exosomes: a novel biomarker in cancer detection. Cell Res 2014;24:766-9.

5. Kahlert C, Melo SA, Protopopov A, Tang J, Seth S, Koch M, et al. Identification of double-stranded genomic DNA spanning all chromosomes with mutated KRAS and p53 DNA in the serum exosomes of patients with pancreatic cancer. J Biol Chem 2014;289:3869-75.

6. Caby MP, Lankar D, Vincendeau-Scherrer C, Raposo G, Bonnerot C. Exosomal-like vesicles are present in human blood plasma. Int Immunol 2005;17:879-87.

7. Pisitkun T, Shen RF, Knepper MA. Identification and proteomic profiling of exosomes in human urine. Proc Natl Acad Sci U S A 2004;101:13368-73.

8. Liga A, Vliegenthart AD, Oosthuyzen W, Dear JW, Kersaudy-Kerhoas M. Exosome isolation: a microfluidic road-map. Lab Chip 2015;15:2388-94.

9. Sheridan C. Exosome cancer diagnostic reaches market. Nat Biotechnol 2016;34:359-60.

10. Weinhold B. Epigenetics: the science of change. Environ Health Perspect 2006;114:A160-7.

11. Esteller M. Epigenetics in cancer. N Engl J Med 2008;358:1148-59.

12. Das PM, Singal R. DNA methylation and cancer. J Clin Oncol

2004;22:4632-42.

13. Ehrlich M. DNA methylation in cancer: too much, but also too little. Oncogene 2002;21:5400-13.

14. Kulis M, Esteller M. DNA methylation and cancer. Adv Genet 2010;70:27-56.

15. Feinberg AP, Vogelstein B. Hypomethylation distinguishes genes of some human cancers from their normal counterparts. Nature 1983;301:89-92.

16. Wan Y, Liu B, Lei H, Zhang B, Wang Y, Huang H, et al. Nanoscale extracellular vesicle-derived DNA is superior to circulating cell-free DNA for mutation detection in early-stage non-small-cell lung cancer. Ann Oncol 2018;29:2379-83.

17. Bernard V, Kim DU, San Lucas FA, Castillo J, Allenson K, Mulu FC, et al. Circulating Nucleic Acids Are Associated With Outcomes of Patients With Pancreatic Cancer. Gastroenterology 2019;156:108-18 e4.

APPENDICES

Supplementary Figure 1A

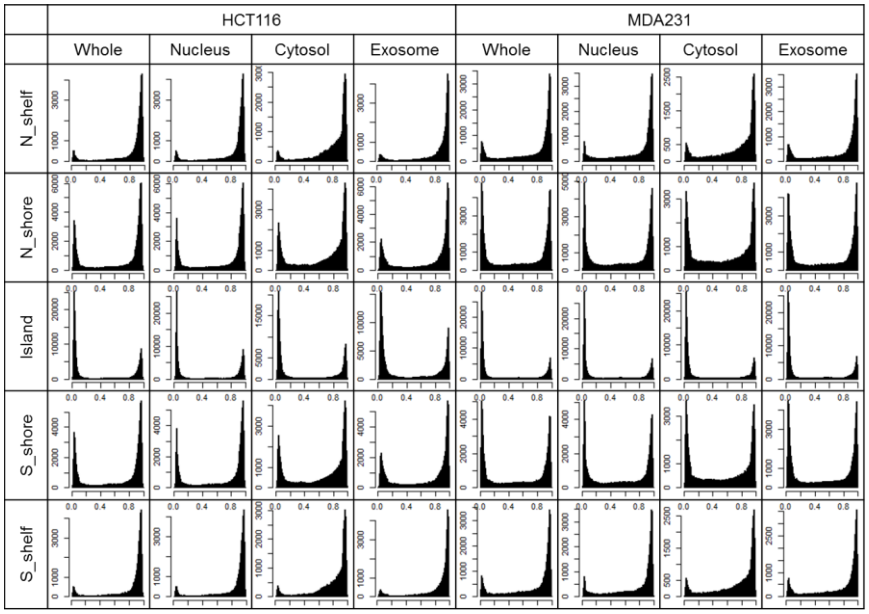

Supplementary Figure 1B

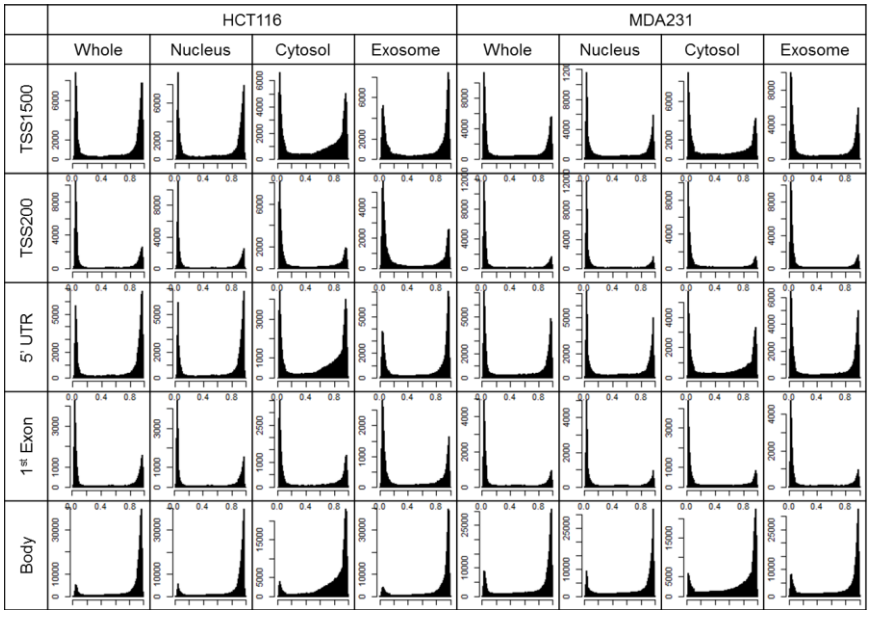

Supplementary Figure 3

A.

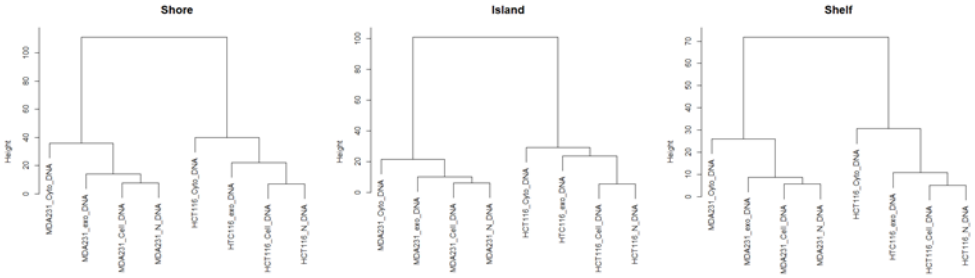

B.

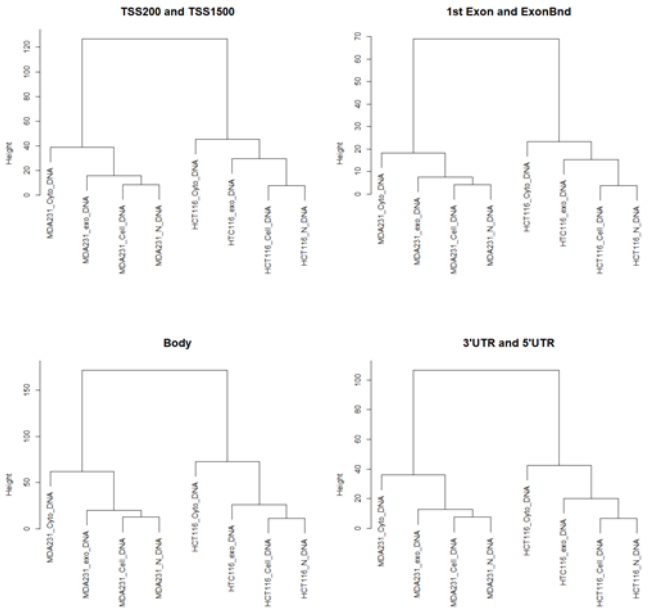

Supplementary Figure 4

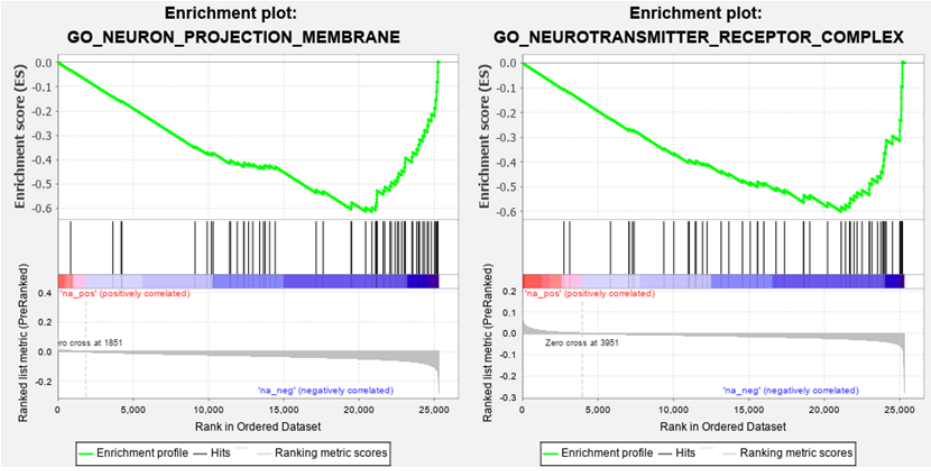

Supplementary Table 1

NAME	SIZE	ES	NES	NOM p-val	FDR q-val	FWER p-val	RANK AT MAX	LEADING EDGE
GO_INTRINSIC_COMPONENT_OF_PEROXISOMAL_MEMBRANE	15	0.430794	1.754474	0.027027	0.366884	0.061	14396	tags=100%, list=67%, signal=232%
GO_SMN_SM_PROTEIN_COMPLEX	17	0.304675	1.18277	0.1875	1	0.567	17582	tags=100%, list=70%, signal=328%
GO_RESPIRATORY_CHAIN_COMPLEX_IV	16	0.304395	1.174784	0.121212	1	0.6	11	tags=6%, list=0%, signal=6%
GO_DNA_REPLICATION_FACTOR_A_COMPLEX	15	0.29246	1.126231	0.3	1	0.671	17890	tags=100%, list=71%, signal=342%
GO_ANAPHASE_PROMOTING_COMPLEX	21	0.219842	1.104453	0.333333	1	0.713	19726	tags=100%, list=78%, signal=456%
GO_NUCLEAR_EXOSOME_RNASE_COMPLEX	15	0.304962	1.101337	0.340909	1	0.717	7191	tags=87%, list=28%, signal=121%
GO_ENDOPLASMIC_RETICULUM_QUALITY_CONTROL_COMPARTMENT	22	0.245772	1.084925	0.222222	1	0.748	10	tags=5%, list=0%, signal=5%
GO_INTRINSIC_COMPONENT_OF_MITOCHONDRIAL_OUTER_MEMBRANE	21	0.238671	1.063707	0.3	1	0.774	19503	tags=100%, list=77%, signal=437%
GO_MITOCHONDRIAL_SMALL_RIBOSOMAL_SUBUNIT	28	0.226029	1.062123	0.363636	0.922935	0.775	18738	tags=100%, list=74%, signal=388%
GO_ENDOPLASMIC_RETICULUM_TUBULAR_NETWORK	19	0.229342	1.014906	0.34375	0.988133	0.832	16164	tags=95%, list=64%, signal=263%
GO_RNA_POLYMERASE_II_CORE_COMPLEX	15	0.267168	0.992483	0.444444	1	0.883	18529	tags=100%, list=73%, signal=374%
GO_SEX_CHROMOSOME	25	0.241259	0.977242	0.5	0.96812	0.875	19186	tags=100%, list=76%, signal=414%
GO_COPI_COATED_VESICLE_MEMBRANE	19	0.223428	0.956083	0.464546	0.959053	0.894	19635	tags=100%, list=78%, signal=447%
GO_DNA_HELICASE_COMPLEX	15	0.252573	0.94449	0.511628	0.932496	0.901	15	tags=7%, list=0%, signal=7%
GO_CYTOSOLIC_SMALL_RIBOSOMAL_SUBUNIT	42	0.208693	0.892299	1	1	0.93	20012	tags=100%, list=79%, signal=479%
GO_EXON_EXON_JUNCTION_COMPLEX	19	0.220404	0.882629	0.676471	0.967053	0.934	65	tags=11%, list=0%, signal=11%
GO_EXORIBONUCLEASE_COMPLEX	25	0.195078	0.867307	0.666667	0.947939	0.938	16188	tags=96%, list=64%, signal=267%
GO_CYTOCHROME_COMPLEX	28	0.216295	0.84282	0.571429	0.948882	0.947	11	tags=4%, list=0%, signal=4%
GO_INO80_TYPE_COMPLEX	25	0.199762	0.803026	0.692308	0.978698	0.96	15	tags=4%, list=0%, signal=4%
GO_CYTOPLASMIC_SIDE_OF_ENDOPLASMIC_RETICULUM_MEMBRANE	15	0.221851	0.798257	0.939394	0.940934	0.961	19679	tags=100%, list=78%, signal=451%
GO_SMALL_NUCLEOLAR_RIBONUCLEOPROTEIN_COMPLEX	26	0.203828	0.751308	0.764706	0.970525	0.969	13811	tags=92%, list=55%, signal=203%
GO_MEDIATOR_COMPLEX	30	0.186738	0.736399	1	0.948493	0.971	20566	tags=100%, list=81%, signal=535%
GO_TRANSLATION_PREINITIATION_COMPLEX	18	0.166614	0.657273	0.942857	0.985268	0.98	21070	tags=100%, list=83%, signal=600%
GO_ROUGH_ENDOPLASMIC_RETICULUM_MEMBRANE	25	0.13217	0.522206	1	0.994491	0.985	13607	tags=88%, list=54%, signal=190%
GO_SMALL_RIBOSOMAL_SUBUNIT	71	0.208933			1	0	20012	tags=100%, list=79%, signal=479%
GO_ORGANELLAR_RIBOSOME	86	0.126138			1	0	19281	tags=97%, list=76%, signal=405%
GO_RIBOSOMAL_SUBUNIT	181	0.099247			1	0	22788	tags=100%, list=90%, signal=1007%

Supplementary Table 2

NAME	SIZE	ES	NES	NOM p-val	FDR q-val	FWER p-val	RANK AT MAX	LEADING EDGE
GO_CATENIN_COMPLEX	28	-0.73856	-2.08514	0	0	0	1915	tags=54%, list=8%, signal=58%
GO_NEURON_PROJECTION_MEMBRANE	58	-0.61341	-1.8797	0	7.64E-04	0.004	4448	tags=57%, list=18%, signal=69%
GO_DENDRITE_MEMBRANE	42	-0.61891	-1.84088	0	0.0027	0.017	4855	tags=57%, list=19%, signal=71%
GO_GLYCOPROTEIN_COMPLEX	19	-0.6814	-1.83669	0	0.002587	0.019	843	tags=37%, list=3%, signal=38%
GO_INTRINSIC_COMPONENT_OF_POSTSYNAPTIC_MEMBRANE	120	-0.55272	-1.78458	0	0.005966	0.049	7066	tags=64%, list=28%, signal=89%
GO_INTRINSIC_COMPONENT_OF_SYNAPTIC_MEMBRANE	103	-0.54054	-1.77834	0	0.006458	0.059	6900	tags=61%, list=27%, signal=84%
GO_INTRINSIC_COMPONENT_OF_POSTSYNAPTIC_DENSITY_MEMBRANE	52	-0.57624	-1.76843	0	0.00724	0.074	6878	tags=65%, list=27%, signal=90%
GO_INTRINSIC_COMPONENT_OF_PRESYNAPTIC_MEMBRANE	82	-0.55983	-1.76669	0	0.00684	0.077	6900	tags=63%, list=27%, signal=87%
GO_POSTSYNAPTIC_DENSITY_MEMBRANE	80	-0.55857	-1.75818	0	0.007304	0.09	5957	tags=61%, list=24%, signal=80%
GO_INTRINSIC_COMPONENT_OF_POSTSYNAPTIC_SPECIALIZATION_MEMBRANE	75	-0.55773	-1.75401	0	0.007329	0.097	6878	tags=64%, list=27%, signal=88%
GO_POSTSYNAPTIC_SPECIALIZATION_MEMBRANE	106	-0.54951	-1.75304	0	0.00694	0.099	5957	tags=60%, list=24%, signal=79%
GO_NEUROTRANSMITTER_RECEPTOR_COMPLEX	53	-0.57758	-1.75141	0	0.006669	0.102	6440	tags=62%, list=22%, signal=79%
GO_GABA_ERGIC_SYNAPSE	70	-0.56084	-1.73035	0	0.008763	0.136	6507	tags=64%, list=26%, signal=86%
GO_CATION_CHANNEL_COMPLEX	214	-0.51918	-1.72875	0	0.008686	0.141	7334	tags=62%, list=29%, signal=87%
GO_SODIUM_CHANNEL_COMPLEX	26	-0.61666	-1.7251	0	0.008626	0.149	7334	tags=81%, list=29%, signal=114%
GO_PRESYNAPTIC_MEMBRANE	156	-0.52851	-1.72194	0	0.008623	0.155	7398	tags=62%, list=29%, signal=86%
GO_CALCIUM_CHANNEL_COMPLEX	62	-0.55492	-1.70236	0	0.01119	0.206	6815	tags=65%, list=27%, signal=88%
GO_PRESYNAPTIC_ACTIVE_ZONE_CYTOPLASMIC_COMPONENT	16	-0.84738	-1.69762	0.001044	0.011428	0.221	7360	tags=75%, list=29%, signal=106%
GO_POTASSIUM_CHANNEL_COMPLEX	96	-0.52469	-1.66644	0	0.017273	0.334	5440	tags=55%, list=22%, signal=69%
GO_POSTSYNAPTIC_MEMBRANE	328	-0.49252	-1.66446	0	0.017019	0.341	4839	tags=47%, list=20%, signal=57%
GO_VOLTAGE_GATED_CALCIUM_CHANNEL_COMPLEX	41	-0.56333	-1.66319	0	0.016867	0.346	6815	tags=68%, list=27%, signal=93%
GO_SYNAPTIC_MEMBRANE	432	-0.48197	-1.64356	0	0.020496	0.41	6660	tags=53%, list=26%, signal=70%
GO_SARCOLEMMA	133	-0.50301	-1.63709	0	0.021758	0.447	6887	tags=55%, list=27%, signal=75%
GO_TRANSPORTER_COMPLEX	324	-0.484	-1.63079	0	0.022786	0.48	7334	tags=57%, list=29%, signal=79%

Supplementary Table 3. Pyrosequencing methylation assay Primers

Candidate	Primer	Sequence
cg15696408	Forward	GTTTATTTTAGAATGAGGTGGTTAGAG
	Reverse	AAACCTACCCCCCCCATCCTAATA
(HCT116)	Sequence	GGAAGGAGAGTTGTAGGGGA
cg00490885	Forward	ATGTAGAAGGTATAGGGATTAGTTT
	Reverse	TAACCCCAAACCCATTCCACCTTA
(MDA231)	Sequence	TTTTTTTGAGGTATTATATTTATTG

ABSTRACT (IN KOREAN)

엑소좀 디엔에이의 후성유전학적 특성과 임상적 효용성

< 지도교수 김한상 >

연세대학교 대학원 의과학과

김 두 아

엑소좀은 30-150 nm 크기의 엔도좀 유래 세포 외 소포체로 세포 간 통신 및 유전 정보 전달에 관여한다. 엑소좀은 이중 가닥 DNA를 포함한 다양한 유형의 핵산을 포함한다. 비정상적인 DNA 메틸화 변화가 암 검출에 유용한 암 바이오 마커가 될 수 있지만, 엑소좀 DNA의 후성 유전학적 특성에 대해 밝혀져야 할 것이 많다. 이 연구에서는 Infinium MethylationEPIC BeadChip을 사용하여 게놈 전체 메틸화 프로파일링을 수행하여 각각 MDA231 및 HCT116 암 세포주에서 파생된 핵, 세포질 및 엑소좀 DNA의 853,307 개 CpG 부위의 메틸화 상태를 조사했다. 인접한 CGI에 기반한 메틸화 프로파일의 계층적 clustering은 세 가지 범주 (섬, 선반 및 해안)로 분리되어 서로 다른 세포 분획 간의 메틸화 프로파일이 대부분 일치함을 보여주었다. 핵 DNA와 엑소좀 DNA의 피어슨 상관 계수는 0.98 (HCT-116)과 0.99 (MDA-MB-231)로 암세포에서 추출한 엑소좀 DNA의 메틸화 분석이 암 검출에 적용될 수 있음을 시사한다. 종양 미세 환경에서 후성 유전학적 변형을 갖는 엑소좀 DNA의 역할을 명확히 하기 위해서는 추가 분석이 필요하다.

핵심되는 말: 엑소좀, 후성유전학, DNA 메틸레이션